# Synchronously pumped optical parametric oscillator based on periodically poled MgO-doped lithium niobate

Kang-Jeon Han<sup>1</sup>, Dong-Wook Jang<sup>1</sup>, Ji-Hee Kim<sup>1</sup>, Chang-Ki Min<sup>2</sup>, Tai-Ha Joo<sup>2</sup>, Yong-Sik Lim<sup>3</sup>, Donghan Lee<sup>1</sup>, and Ki-Ju Yee<sup>1\*</sup>

<sup>1</sup>Department of Physics, Chungnam National University, Daejeon 305-764, Korea
<sup>2</sup>Department of Chemistry, Pohang University of Science and Technology, Pohang 790-784, Korea
<sup>3</sup>Department of Applied Physics, Konkuk University, Chungju, Chungbuk 380-701, Korea
\*Corresponding author: kyee@cnu.ac.kr

**Abstract:** We demonstrate a room-temperature operation of the near-infrared femtosecond optical parametric oscillator based on MgO-doped stoichiometric periodically-poled lithium niobate, which is synchronously pumped by a Kerr-lens mode-locked Ti:sapphire laser. Wide tunability in the range from 0.98  $\mu$ m to 1.50  $\mu$ m was enabled for a single set of cavity mirrors by incorporating a BK7 window as an output coupler. For the output coupling ratio of 3.7%, the threshold pumping power of 460 mW and the slope power conversion efficiency of 37% were achieved. By controlling dispersion values with intra-cavity prisms, femtosecond pulses as short as 66 fs could be obtained.

©2008 Optical Society of America

**OCIS codes:** (190.4410) Nonlinear optics, parametric processes; (190.4970) Parametric oscillators and amplifiers.

### References and links

- D. C. Edelstein, E. S. Wachman, C. L. Tang, "Broadly tunable high repetition rate femtosecond optical parametric oscillator," Appl. Phys. Lett. 54, 1728-1730 (1989).
- R. J. Ellingson and C. L. Tang, "High-power, high-repetition-rate femtosecond pulses tunable in the visible," Opt. Lett. 18, 438-440 (1993).
- 3. H. M. van Driel, "Synchronously pumped optical parametric oscillators," Appl. Phys. B 60, 411-420 (1995).
- S. W. McCahon, S. A. Anson, D.-J. Jang, M. E. Flatté, T. F. Boggess, D. H. Chow, T. C. Hasenberg, and C. H. Grein, "Carrier recombination dynamics in a (GaInSb/InAs)/AlGaSb superlattice multiple quantum well," Appl. Phys. Lett 68, 2135-2137 (1996).
- Y. Okawachi, M. A. Foster, J. E. Sharping, A. L. Gaeta, Q. Xu, and M. Lipson, "All-optical slow-light on a photonic chip," Opt. Express 14, 2317-2322 (2006).
- J. A. Armstrong, N. Bloembergen, J. Ducuing, and P. S. Pershan, "Interactions between Light Waves in a Nonlinear Dielectric," Phys. Rev. 127, 1918-1939 (1962).
- L. E. Myers, R. C. Eckardt, M. M. Fejer, R. L. Byer, W. R. Bosenberg, and J. W. Pierce, "Quasi-phase-matched optical parametric oscillators in bulk periodically poled LiNbO3," J. Opt. Soc. Am. B 12, 2102-(1995).
- T. Kartaloğlu, K. G. Köprülü, O. Aytür, M. Sundheimer, and W. P. Risk, "Femtosecond optical parametric oscillator based on periodically poled KTiOPO<sub>4</sub>," Opt. Lett. 23, 61-63 (1998).
- K. C. Burr, C. L. Tang, M. A. Arbore, and M. M. Fejer, "Broadly tunable mid-infrared femtosecond optical parametric oscillator using all-solid-state-pumped periodically poled lithium niobate," Opt. Lett. 22, 1458-1460 (1997).
- Y. Furukawa, K. Kitamura, S. Takekawa, A. Miyamoto, M. Terao, and N. Suda, "Photorefraction in LiNbO<sub>3</sub> as a function of [Li]/[Nb] and MgO concentrations," Appl. Phys. Lett. 77, 2494-2496 (2000).
- T. Andres, P. Haag, S. Zelt, J. P. Meyn, A. Borsutzky, R. Beigang, and R. Wallenstein, "Synchronously pumped femtosecond optical parametric oscillator of congruent and stoichiometric MgO-doped periodically poled lithium niobate," Appl. Phys. B 76, 241-244 (2003).
- H. P. Li, D. Y. Tang, S. P. Ng, and J. Kong, "Temperature-tunable nanosecond optical parametric oscillator based on periodically poled MgO:LiNbO3," Opt. Laser Technol. 38, 192-195 (2006).

## 1. Introduction

Synchronously pumped femtosecond optical parametric oscillators (OPO), enabling the ultrashort light sources tunable in the near- and mid-infrared as well as in the visible [1-3], have been proved to be attractive sources for laser applications in such fields like time-resolved spectroscopy and coherent light-matter interactions [4-5]. Regarding the phase-matching method for enhanced efficiency of the nonlinear parametric down conversion, quasi-phase matching (QPM) technique is taking an increasing share over the conventional birefringent phase matching (BPM) [6]. In the QPM, the phase mismatch occurring due to the dispersed group velocity with wavelength inside a medium, is relaxed by an artificial periodicity of the poling direction, as was demonstrated for periodically poled lithium niobate (PPLN) and KTP [7,8]. For the QPM, the parametric conversion condition can be manipulated with the poling period in the fabrication, and it can also utilize the largest nonlinear coefficients of the crystal.

PPLN is one of the most widely used crystals as the OPO medium nowadays, because of the large nonlinear optical coefficient  $d_{33}$  accessible for all three involving waves being polarized in extraordinary direction ( $e \rightarrow e + e$ ) of the crystal [9]. However, the QPM suffers from the low threshold for photorefractive damage, generally requiring crystal heating up to 100 °C for the OPO operations. Recently, magnesium-oxide (MgO) doping was found to decrease tremendously the photorefractive effect [10], and the OPO operation at room temperature was demonstrated by using the MgO-doped crystal [11].

In this paper, we demonstrate the operation of a novel femtosecond OPO based on MgO-doped stoichiometric PPLN, which is synchronously pumped by a Kerr-lens mode-locked Ti:sapphire laser. Utilizing the ring-type cavity configuration with dispersion manageable prism pairs, broadly tunable operation from 0.98 to 1.5  $\mu$ m in the signal branch is demonstrated for a single set of cavity mirrors. The wavelength tunability as a function of the pump wavelength, and spectral and temporal characteristics of output pulses are discussed depending on the total intra-cavity dispersion.

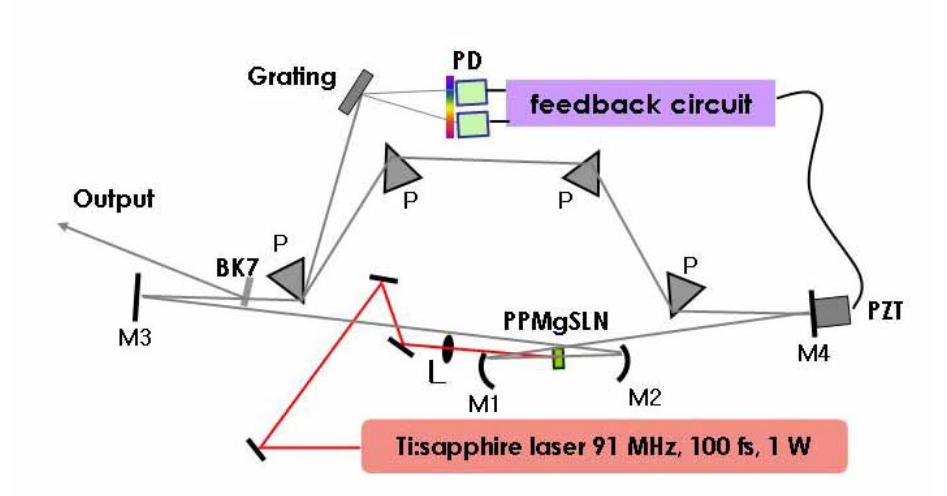


Fig. 1. Schematic diagram of the PPMgSLN based femtosecond OPO with a ring-type configuration. PPMgSLN, periodically poled lithium niobate doped with 1.3 mol % MgO; L, 15 cm focal length plano-convex lens, M1&M2, spherical mirrors with 15 cm radius of curvature; M3&M4, flat mirrors; P, SF11 equilateral prism; PZT, piezoelectric actuator; PD, photodiode; BK7, transparent window used for an output coupler.

# 2. Experiments

Commercial periodically-poled stoichiometric lithium niobate crystal (PPMgSLN), doped with 1.3 mol % MgO for reduced photorefractivity, was used for easy operation at room temperature. The crystal length along the optical path was 0.5 mm, containing 7 different poling periods from 20.5 to 21.1  $\mu$ m with a step of 0.1  $\mu$ m. To minimize reflection losses, both sides of the crystal were anti-reflection coated for the pump (780-850 nm) and signal (1.0-1.5  $\mu$ m) wavelength ranges. The synchronous pumping source was a femtosecond modelocked Ti:sapphire oscillator with an average power of 1 W and a repetition rate of 91 MHz. The pump pulse was tunable between 750 to 850 nm with the spectral bandwidth of 10 nm FWHM and pulse duration around 100 fs. We adopted a noncollinear pumping scheme so that the pump beam passes by the concave mirror with an external deviation angle of 2.3°, corresponding to the internal deviation angle of 1.1° relative to the signal path. The noncollinear pumping allows the best use of the broadband high reflectors in the signal branch, and is advantageous in picking out the idler beam.

Both linear- and ring-type configurations can be used for the OPO cavity. The important advantages of the ring-type cavity are the absence of spatial hole burning in gain medium, unidirectional output, and optical isolation of the OPO pulse from back reflection into the pump laser. Although the ring-type configuration supports oscillation in both clockwise and counterclockwise directions, the parametric gain of OPO is exclusively in the direction of the pump pulse. Therefore, we chose a ring cavity configuration to get a lower threshold pumping power and a better slope efficiency. A schematic of the OPO cavity is shown in Fig. 1. The cavity is composed of a pair of concave mirrors with a 15 cm radius of curvature which are folding the PPMgSLN crystal, a pair of plat mirrors, and a four-prism sequence of SF11 dispersive prisms to control the intra-cavity dispersion. The dielectric coating for cavity mirrors were designed to have a high reflectivity of R>99.8%, and a small negative group velocity dispersion (GVD) in the signal branch to come in pairs to compensate for the residual oscillations in the GVD. As an output coupler, BK7 window of 6 mm thickness was ARcoated at a side and placed inside the OPO ring cavity. This transparent window has two main advantages over conventional dielectric output couplers. First, the coupling ratio can be controlled within a certain value by rotating the window relative to the beam direction. Second, the coupling ratio is almost uniform over the wide spectral range. Thus, unidirectional ring cavity in combination with the BK7 window as an output coupler provides an ideal cavity layout for the efficient widely tunable OPO.

The spectral and power fluctuations induced by unstable cavity parameters were reduced by incorporating a proportional-integral feedback control loop that stabilize the signal spectrum by cavity-length adjustment with a piezoelectric transducer. The output spectrum was measured by an InGaAs array spectrometer, and the temporal shape of signal pulses was studied by measuring the second harmonic generation of two cross-correlated, time-delayed beams in the BBO crystal.

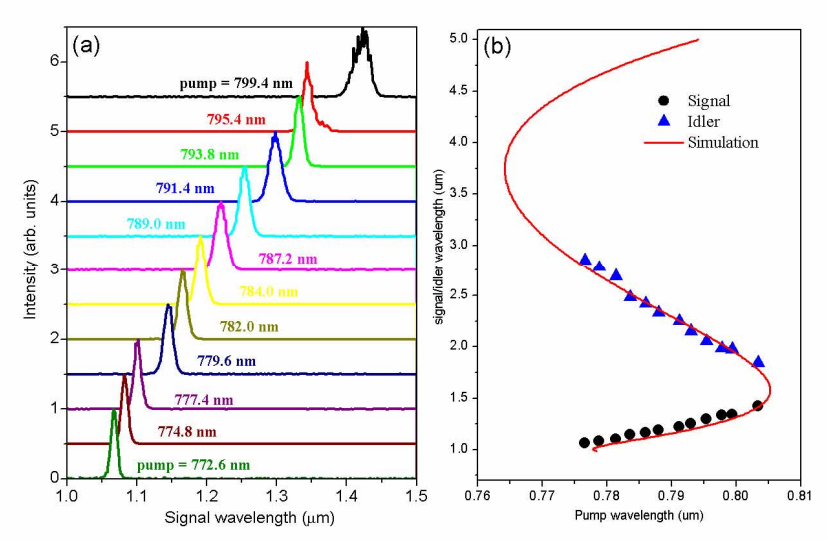


Fig. 2. (a). Signal spectrum obtained for different pump wavelengths for a poling period of  $\Lambda$ =20.8  $\mu$ m at room temperature. (b). Signal and calculated idler wavelengths and calculated tuning curve for the signal and the idler with a QPM period of  $\Lambda$ =20.8  $\mu$ m at room temperature.

## 3. Results and discussion

The quasi-phase matching condition for signal  $(\omega_s)$ /idler  $(\omega_i)$  wavelengths depends on various parameters such as poling period  $(\Lambda)$ , crystal temperature, and the pump wavelength  $(\omega_p)$ . With a fixed poling period of  $\Lambda$ =20.8  $\mu m$  at room temperature, we can tune the signal wavelength from 0.98 to 1.5  $\mu m$  by changing the pump wavelength from 777 to 802 nm. Figure 2(a) shows the signal spectrum obtained for different center wavelengths of pump pulse. In the non-collinear pumping geometry, the phase matching condition is also influenced by the propagation angle  $(\theta)$  between the pump and the signal beam, and therefore, the phase matching condition is modified to the followings,

$$(k_s + \frac{2\pi}{\Lambda}) \times \sin \theta = k_i \times \sin \theta', \quad k_p = (k_s + \frac{2\pi}{\Lambda}) \times \cos \theta + k_i \times \cos \theta', \tag{1}$$

where  $k_p$ ,  $k_s$ ,  $k_i$  and  $\theta'$  correspond to the wave vector of the pump, signal, idler, and the propagation angle of the idler beam, respectively. From the relations of Eq. (1) and the energy conservation ( $\omega_{pu} = \omega_s + \omega_i$ ), signal and idler wavelengths can be calculated to give the solid line in Fig. 2(b), which is in a good agreement with the experimental measurements from Fig. 2(a). We note that the points for the idler wavelength was deduced from the energy conservation, and the refractive index coefficients in the Sellmeier equation for the PPMgSLN were interpolated from the coefficients for a 5% MgO-doped crystal [12]

Besides the phase matching condition, synchronous pumping condition is important for deciding the signal/idler wavelength within the phase-matching tolerance. As shown in Fig. 3(a), the signal wavelength can be continuously tuned over 500 nm by adjusting the cavity length as well as the pump wavelength. At a fixed pump wavelength, the signal wavelength can be tuned over 200 nm by just adjusting the cavity length. The signal power shown in Fig. 3 for each pump wavelength is related to the phase mismatch, where the signal is determined mainly by the synchronization with the repetition rate of the pump pulse. And the maximum power for each pump wavelength occurs for the signal wavelength which satisfies both the optimal quasi phase matching and the synchronized condition to the pump repetitions.

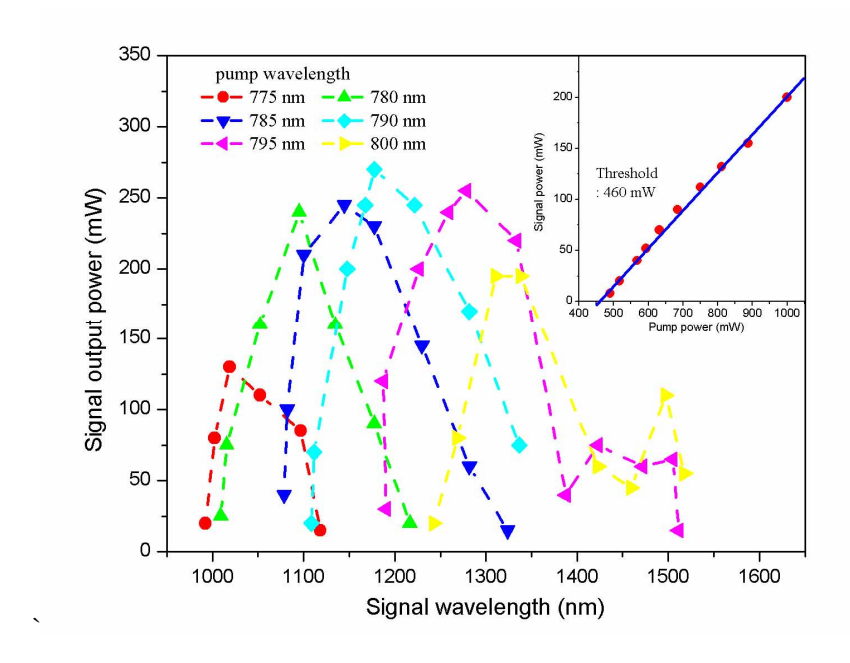


Fig. 3. The signal output power as a function of the signal wavelength which is continuously tunable by adjusting the cavity length and changing the pump wavelength. The inset shows the signal power as a function of pump intensity for fixed signal and pumping wavelengths of  $0.792~\mu m$  and  $1.225~\mu m$ , respectively.

For a 3.7% output coupling of the BK7 window, the signal power at around 1.2  $\mu$ m is as high as 280 mW for 1.1 W pump power. Relatively high power is sustained in signal range of 1.05 – 1.35  $\mu$ m. We note that the reduced power around 1.4  $\mu$ m is attributed by the water vapor absorption, which may be recovered by nitrogen purging. Shown in the inset of Fig. 3 is the signal power as a function of the pump power obtained at fixed signal and pump wavelengths of 0.792  $\mu$ m and 1.225  $\mu$ m, respectively. For 3.7% output coupling, the threshold pump power was 460 mW, with the power slope efficiency being 37% (57% quantum slope efficiency). For a smaller output coupling ratio, both the threshold pump power and the slope efficiency has decreased.

Because of the fixed roundtrip time set by the synchronously pumping, the pulse duration and spectrum of signal pulses from a synchronous pumped OPO are dominated by the intracavity dispersion which the pulse experiences during the round-trip. We have investigated how the pulse width and its spectrum of a femtosecond OPO signal depend on the intra-cavity dispersion, by controlling the insertion of intra-prisms. In changing the length of the cavity for a given intra-cavity dispersion, only those signal wavelengths whose dispersion-related roundtrip times are synchronized with the repetition rate of the master oscillator will be selected. For example, for a positive (negative) dispersion, red-shift (blue-shift) light precedes the blue-shift (red-shift) light. In order to achieve synchronization with the pump pulses, the red-shift (blue-shift) light for a positive (negative) dispersion should be adjusted to take a longer roundtrip time by lengthening the physical cavity length of the oscillator, which is well consistent with the experimental results as shown in the insets of Fig. 4. The slope of the profile in the insets in Fig. 4 relates to the spectral width of the pulses supported by the resonator. Near zero intra-cavity dispersion, the slope becomes steep and the pulse spectra become broader. From the reversal spectral change between positive and negative intra-cavity dispersion as a function of cavity length mismatch, we can roughly estimate the sign and magnitude of the intra-cavity dispersion.

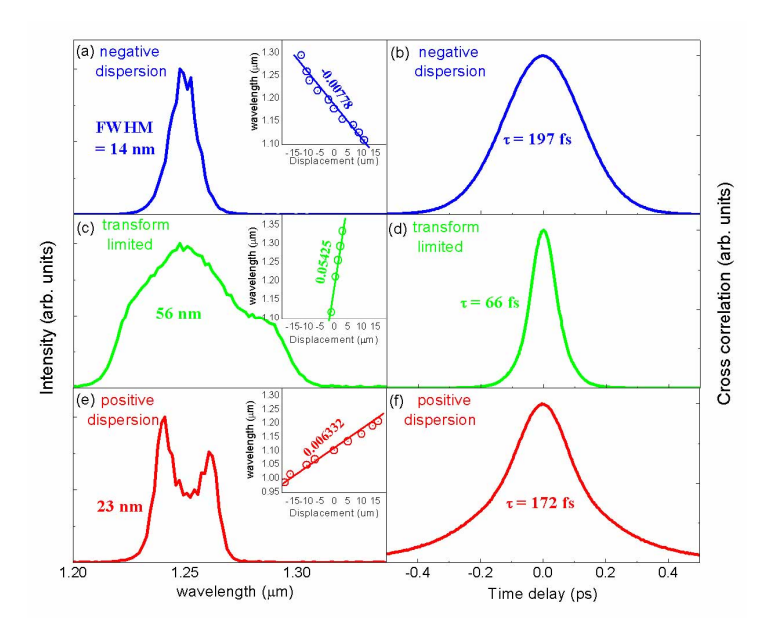


Fig. 4. The output pulse spectrum ((a), (c), (e)) and cross correlation intensity as a function of time delay ((b), (d), (f)) for the case of transformed limited, negative dispersion, and positive dispersion. The insets of Fig. 4(a), 4(c), 4(e) depicts the change of the signal wavelength as a function of cavity length displacement.

Figure 4 shows the signal spectrum and pulse duration for negative, positive, and nearzero intra-cavity dispersions. At the signal wavelength of 1.25 µm, the shortest pulse duration of 66 fs was obtained at near-zero dispersion, and the spectral width was obtained to be 56 nm FWHM, corresponding to a time-bandwidth product of  $\Delta v \Delta \tau = 0.712$ . As depicted in Fig. 4, the pulse duration becomes longer and the spectral width becomes narrower as the dispersion deviates from zero towards a negative or positive value. Nonetheless, when operating at zero dispersion, the spectra and the power level are sensitive to minute cavity length fluctuation.

# 4. Conclustion

We reports a broadly tunable femtosecond OPO based on a stochiometric MgO doped periodically poled lithium niobate synchronously pumped by a Kerr-lens mode-locked Ti:sapphire laser. With a BK7 window as an output coupler, the output signal pulses can be continuously tuned from 0.98 to 1.5 µm by tuning only the center wavelength of the pump pulses. The threshold pump power of 460 mW, and the slope conversion efficiency of 37% are obtained, and the signal power of around 280 mW could be reached at a pump power of 1.1 W. By controlling the intra-cavity dispersion close to zero, signal pulses as short as 66 fs are demonstrated, while the pulse duration becomes longer for negative or positive dispersions. Although the pulse duration is longer for negative or positive dispersions, the signal spectrum is found to be less sensitive to the cavity length fluctuations.

# Acknowledgments

This work was supported by the Ministry of Commerce, Industry and Energy of Korea through the Industrial Technology Infrastructure Building Program, and by the Korean Science and Engineering Foundation (KOSEF) grant (R01-2007-000-20651-0).